Trends in Life Sciences
An International Peer-reviewed Journal
www.sciencejournal.in

THE SYNTHESIS, EXPERIMENTAL AND THEORETICAL VIBRATIONAL STUDIES ON 1,3-BIS(4-BENZAMIDO) TRIAZENE AT HF AND DFT LEVELS OF THEORY

Fahimeh Garakhani[a], Zahra Asadi[a], Shahla Daneshmehr[b,*], Ladan Edjlali[c], Esmail Vessally[d]
[a] Department of Chemistry, Miyaneh Branch, Islamic Azad University, Miyaneh, Iran
[b] Young Researchers and Elite Club, Tabriz Branch, Islamic Azad University, Tabriz, Iran
[c] Department of Chemistry, Tabriz Branch, Islamic Azad University, Tabriz, Iran
[d] Department of Chemistry, Payame Noor University (PNU), PO BOX 19395-4697, Tehran, Iran
*Corresponding author: shahladaneshmehr@yahoo.com

ABSTRACT
The synthesis, experimental and theoretical vibrational studies were carried out on 1,3-bis(4-benzamido)triazene, at the Hartree Fock (HF) and density functional theory methods (DFT/PBE1PBE) with 6-311+G(2d,p) basis set. The harmonic vibrational wavenumbers of **2** were calculated at the scaled values were compared with the experimental FT-IR spectra. A detailed harmonic vibrational wavenumbers of **2** were reported. The calculated data were in reasonably good agreement with experimental measurements.

KEYWORDS: 1,3-Bis(4-benzamido)triazene; IR; 6-311+G(2d,p)

1. INTRODUCTION

Griess has first synthesized the 1,3-Bisphenyl triazenes (Griess, 1859). The 1,3-Bisphenyl triazenes are compounds that are useful because they have different applications as intermediate compounds in organic synthesis, ligands in transition metal complexes, antibacterial, antileukemic, anticancer and antitripanosomal activities, fluorescence sensors, treatment of tumour diseases, photo-switchable materials and selective electrodes for measurement of the trace amount of mercury ion in the water samples (Enders *et al*., 2004; Erdogdu *et al*., 2009; Iglesias *et al*., 2012; Kimball *et al*., 2002; Melardi *et al*., 2012; Rofouei *et al*., 2012; Sanada *et al*., 2004; Santos *et al*., 2014; Vessally *et al*., 2011). This research demonstrates and disputes the synthesis and characterization of new triazene, 1,3-bis (4-benzamido)triazene, 2, by FT-IR and NMR spectroscopy. Moreover, we compared the experimental results with calculated data using the Hartree-Fock (HF) and density functional theory method (DFT/PBE1PBE) with 6-311+G(2d,p) basis set.

2. EXPERIMENTAL AND THEORETICAL METHODS

2.1. General Method

The melting point was determined in the equipment Gallenkamp. Elemental analysis was performed with Perkin-Elmer 2400 series II. ^{1}H and ^{13}C nuclear magnetic resonance spectra were recorded on a Bruker Avance 300 instrument (300 MHz; $CDCl_3$) with the processing software XWINNMR version 3.1. Chemical shifts are reported on δ scale relative to TMS. The room temperature Fourier transform infrared spectrum of the title compound was recorded in the region 400–4000 cm^{-1} with ±1cm^{-1} resolution using a PerkinElmer spectrum RXI FT-IR spectrometer, utilizing KBr discs.

2.2. Synthesis

4-Aminobenzamide (2.181 g, 16.02 mmol), **1**, was dissolved in a mixture of 20 mL of concentrated HCl and 10 mL of distilled water and the system was cooled to -2°C. Then sodium nitrite (1.429 g, 16.82 mmol) was added under constant stirring. The system was neutralized to a pH of around 7, with sodium carbonate solution. The synthetic route is shown in Scheme 1. The yellow precipitate, separated by filtration, was washed with small amounts of cold water, followed by small amounts of cold ethanol and purified by column chromatography after its adsorption onto silica gel (70/230 mesh) using hexane: ethyl acetate (3:7) as eluent. The microcrystalline product was recrystallized from a hexane: ethyl acetate mixture (1:3). Yellow vitreous bar-shaped crystals were obtained by slow evaporation of the solvent mixture within five days. Yield of 86% (1.75 g, 5.7 mmol) based on taken 2,4-dichloroaniline. Mp. 115-116°C. FT-IR max/cm^{-1}, KBr pellets: 3732 (N−H, amide), 3415 (N−H, amide), 3323 (C−H), 3157 (C−H), 1656(C=C),1604(N−H), 1525(d(C−H), deformation), 1247 (C-N), 1053 (C-O), 743 ((C-Cl), deformation). ^{1}H NMR (300 MHz, dmso-d6/tms) d 12.84 (s, 1H, NH), 7.93-7.29 (m, 8H, Ph), 3.32 (2H, NH), 3.34 (2H, NH). ^{13}C NMR (300 MHz, dmso-d6) d 168 (2C=O), 154.35, 146.54, 130.99, 128.39, 128.34, 127.60, 127.60, 124.61, 120.79, 120.69, 116.45, 116.41 (Ph).

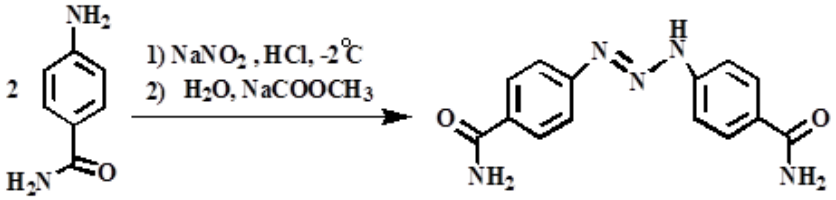

Scheme1. Synthesis of compound **2**.

2.3. Theoretical Methods

All the calculations were carried out with Gaussian 03(Frisch *et al*., 2004). The gradient corrected density functional theory (DFT/PBE1PBE) and Hartree-Fock (HF) with the standard 6-311+G(2d,p) basis set were used. The global minimum of the molecular structure of 1,3-bis(4-benzamido) triazene, **2**, was found and used for vibrational and NMR calculations. The calculated frequencies were scaled by 0.9073 and 0.9944 for HF/6-311+G(2d,p) and PBE1PBE/6-311+G(2d,p) respectively (Merrick *et al*., 2007).

RESULTS AND DISCUSSION

3.1. The geometrical studies

The obtained global minimum of 1,3-bis(4-benzamido) triazene, **2**, was shown in Fig. 1. The geometrical parameters including bond length, bond angle and dihedral angles were presented in Table 1. Since, the crystal structure of **2** is not available, the optimized structure was compared with other similar optimized compounds (Domingues *et al*., 2010). The molecule contains two CO-NH_2 groups and triazeno moiety with two benzene rings. The theoretical amounts of the optimized bond lengths are slightly larger than the experimental amounts since the theoretical calculations belong to the isolated molecule in the gas-phase while the experimental results belong to the molecule in the solid state. Theoretical calculations on the bond angles and bond lengths at the RPBE1PBE level of theory indicated a good correlation with the experimental data compared to HF level of theory. For instance, the optimized bond length of C-C in the phenyl ring occurs in the range of 1.398–1.378 Å at the RPBE1PBE method and 1.390–1.373 Å at the HF method. This is in good agreement with an analogous molecule in where the C-C bond length occurs in the range of 1.401–1.365 Å. According to the experimental values, order of the optimized bond length of the six C–C bonds in the ring are as C_1–C_2 <C_4–C_5 <C_2–C_3 = C_3–C_4 < C_5–C_6 < C_6–C_1. For the calculated RPBE1PBE values, the order of the bond lengths was slightly deviated as C_5–C_6 (1.396Å) > C_1–C_6 (1.394Å) > C_2–C_3 (1.393Å) > C_3–C_4 (1.392Å) >C_1–C_2 (1.382Å) > C_4–C_5 (1.379Å) (Table 1). Moreover, the predicted bond lengths of C_{30}-O_{31}, C_{16}-O_{17} and C_{30}-C_3, C_{16}-C_{13} are 1.216,1.215 and 1.490, 1.493 with RPBE1PBE method, the same bond length are 1.194, 1.193 and 1.493, 1.498 with HF method , the experimental data of named bond are 1.233, 1.233, 1.489, 1.489 respectively. The optimized N-C bond lengths of (N_7–C_6), (N_9–C_{10}) are 1.384 Å, 1.405 Å, (N_{18}–C_{16}) and (N_{32}–C_{30}) are 1.365 Å, using RPBE1PBE method while are 1.384, 1.405, 1.361, 1.363, respectively, using HF method. However, these are slightly different compared to a related molecular structure. The calculated C_6–N_7–N_8 and C_{10}–N_9–N_8 bond angles are 122.6 and 114.6 at RPBE1PBE and HF methods are 122.1 and 115.3, respectively, which are 2.5˚ deviated for both of the bond angle, between RPBE1PBE and their experimental data.

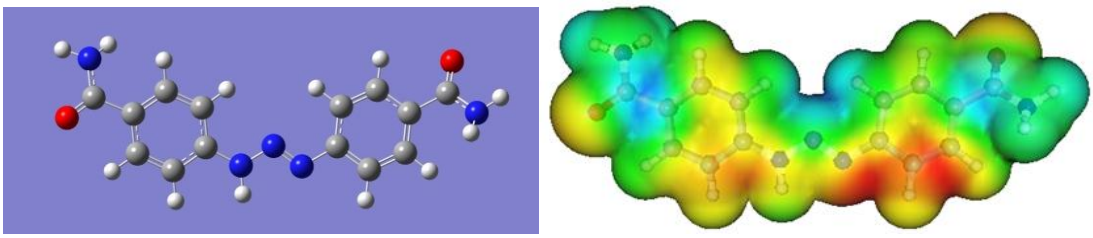

Fig. 1. Optimized structure and calculated 3D molecular electrostatic potential map for 2 with RPBE1PBE/6-311G+(2d,p).

Table 1. Geometrical parameters optimized in 2, bond length (Å), bond angle (°) and dihedral angle (°).

Parameters	X-Ray	PBE1PBE6-311+G(2d,p)	HF/6-311+G(2d,p)
Bond length			
C_{30}–N_{32}	1.335[1]	1.365	1.363
C_{30}–O_{31}	1.233[1]	1.216	1.194
C_{30}–C_3	1.489[1]	1.490	1.493
C_{16}–N_{18}	1.335[1]	1.365	1.361
C_{16}–O_{17}	1.233[1]	1.215	1.193
C_{16}–C_{13}	1.489[1]	1.493	1.498
N_9–C_{10}	1.430[2]	1.405	1.498
N_9–N_8	1.263[2]	1.251	1.214
N_8–N_7	1.340[2]	1.319	1.321
N_7–C_6	1.383[2]	1.384	1.385
C_6–C_5	1.392[2]	1.396	1.390
C_5–C_4	1.366[2]	1.379	1.373
C_4–C_3	1.375[2]	1.392	1.387
C_3–C_2	1.375[2]	1.393	1.385
C_2–C_1	1.365[2]	1.382	1.379
C_1–C_6	1.401[2]	1.394	1.387
C_{10}–C_{15}	1.398[2]	1.398	1.390
C_{15}–C_{14}	1.372[2]	1.378	1.374
C_{14}–C_{13}	1.375[2]	1.395	1.389
C_{13}–C_{12}	1.373[2]	1.392	1.382
C_{12}–C_{11}	1.381[2]	1.384	1.382
C_{11}–C_{10}	1.383[2]	1.392	1.380
$a^{\dagger}$		1.048	1.228
$b^{\dagger}$		-0.061	-0.310
R^2		0.949	0.939
Bond angle			
N_9–N_8–N_7	112.3[2]	112.6	113.8
N_8–N_7–C_6	120.0[2]	122.6	122.1
N_8–N_9–C_{10}	112.1[2]	114.6	115.3
N_9–C_{10}–C_{15}	124.1[2]	125.0	124.6
N_9–C_{10}–C_{11}	115.8[2]	115.5	115.5
N_7–C_6–C_1	120.9[2]	122.0	122.4
N_7–C_6–C_5	119.1[2]	118.2	118.0
N_{32}–C_{30}–O_{31}	121.0[1]	121.6	121.3
N_{32}–C_{30}–C_3	119.0[1]	116.6	117
O_{31}–C_{30}–C_3	119.8[1]	121.7	121.6
N_{18}–C_{16}–O_{17}	121.0[1]	121.7	121.6
N_{18}–C_{16}–C_{13}	119.0[1]	116.4	116.7
O_{17}–C_{16}–C_{13}	119.8[1]	121.7	121.5
C_{16}–C_{13}–C_{12}	123.1[1]	123.5	123.1
C_{16}–C_{13}–C_{14}	118.3[1]	117.4	117.8
C_{13}–C_{14}–C_{15}	119.2[2]	120.9	120.8
C_{13}–C_{12}–C_{11}	120.5[1]	120.3	120.3
C_{14}–C_{15}–C_{10}	119.5[2]	119.8	119.6

$C_{15}–C_{10}–C_{11}$	119.9[2]	119.4	119.7
$C_{10}–C_{11}–C_{12}$	120.5[2]	120.3	120.2
$C_6–C_5–C_4$	120.3[2]	120.0	120.1
$C_6–C_1–C_2$	119.4[2]	119.4	119.4
$C_5–C_4–C_3$	120.5[1]	120.8	120.9
$C_4–C_3–C_2$	118.4[2]	118.5	118.2
$C_3–C_2–C_1$	121.7[1]	121.3	121.5
$C_1–C_6–C_5$	119.8[2]	119.7	119.5
$a^{\ddagger}$		0.975	0.867
$b^{\ddagger}$		3.278	16.21
R^2		0.801	0.785
$^{\ddagger} A_{theo.} = a\, A_{exp.} + b$			
Dihedral angle			
$C_6–N_7–N_8–N_9$	177.5[2]	179.1	176.7
$C_{10}–N_9–N_8–N_7$	-179.9[2]	179.3	179.3
$C_1–C_6–N_7–N_8$	6.38[2]	-1.6	0.2
$C_5–C_6–N_7–N_8$	-173.4[2]	178.7	-179.5
$C_{15}–C_{10}–N_9–N_8$	2.93[2]	-4.6	-10.41
$C_{11}–C_{10}–N_9–N_8$	-175.9[2]	176.26	170.7
$C_2–C_3–C_{30}–N_{32}$	178.0[2]	15.7	17.6
$C_2–C_3–C_{30}–O_{31}$	-2.3[1]	-162.9	-161.0
$C_2–C_3–C_4–C_5$	0.27[2]	-1.0	-1.1
$C_2–C_1–C_6–C_5$	0.74[2]	-0.6	-0.6
$C_6–C_1–C_2–C_3$	-1.18[2]	0.24	0.3
$C_6–C_5–C_4–C_3$	-0.7[2]	0.65	0.8
$C_4–C_3–C_{30}–N_{32}$	-2.6[1]	-165.3	-163
$C_4–C_3–C_{30}–O_{31}$	176.9[1]	16.0	17
$C_{14}–C_{13}–C_{16}–N_{18}$	178.0[1]	163.2	160
$C_{l2}–C_{13}–C_{16}–N_{18}$	-2.65[1]	-17.9	-21
$C_{14}–C_{13}–C_{16}–O_{17}$	-2.3[1]	-18.0	-20
$C_{l2}–C_{13}–C_{16}–O_{17}$	176.9[1]	-160.7	157.7
$C_{15}–C_{14}–C_{13}–C_{16}$	178.9[1]	-179.9	179.9
$C_{15}–C_{14}–C_{13}–C_{12}$	-0.89[2]	1.16	1.29
$C_{15}–C_{10}–C_{11}–C_{12}$	-1.04[2]	0.9	1.3
$C_{10}–C_{11}–C_{12}–C_{13}$	0.5[2]	-0.3	-0.6
$C_{11}–C_{12}–C_{13}–C_{16}$	0.27[1]	-179.4	-179
$C_{11}–C_{12}–C_{13}–C_{14}$	0.48[2]	-0.6	-0.6
(1) 1-(2-fluorophenyl)-3-(4-amido phenyl) triazene (2) 1,3 bis (4-nitrophenyl)triazene			

3.2. FT-IR spectroscopy

The title compound consists of 34 atoms, and therefore it has 96 normal modes of vibrations. Of the 96 normal modes of vibrations, 63 modes of vibrations are in the plane and remaining 34 are out of plane. The bands that are in the plane of the molecule are represented as A' and out-of-plane as A''. Thus the 96 normal modes of vibrations of 2 are distributed as $\Gamma_{Vib} = 61A' + 34A''$. In agreement with C_S symmetry all the 96 fundamental vibrations are not active in IR absorption. The harmonic-vibrational frequencies calculated for 2 at HF and DFT (PBE1PBE) levels using the triple split valence basis set along with the diffuse and polarization functions, 6-311+G(2d,p). Computed and experimental FT-IR spectra are shown in Figure 2. Observed FT-IR frequencies for various modes of vibrations concerning the assignment has been presented in the (Table 2) Comparison of frequencies calculated at HF with the experimental values shows over estimation of the calculated vibrational state due to the inattention of anharmonicity in the real

system. DFT includes electron correlation, for this reason, certain extends make the frequency value smaller in the comparison with the HF frequency data.

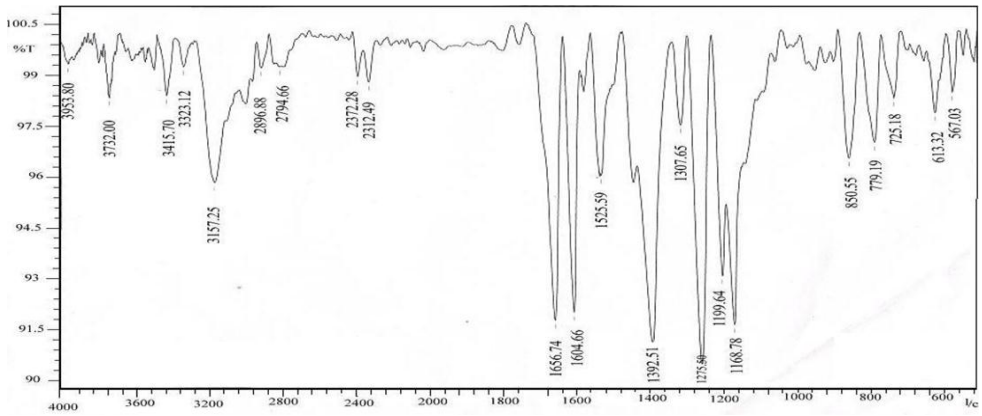

Fig. 2. FT-IR spectra of 1,3-bis (4-amidophenyl)triazene.

Table 2. Observed, PBE1PBE/6-311+G (2d,p) and HF /6-311+G (2d,p) level calculated vibrational frequencies of 2.

S. No.	Symmetry species C_S	Observed frequency	Calculated frequency				Vibrational Assignments	%PED
		FT-IR	PBE1PBE/6-31+G(2d,p)		**HF/6-311+G(2d,p)**			
			Unscaled	Scaled	Unscaled	Scaled		
1	A′	-	3745	3724	3930	3565	(N-H) υ	**58**
2	A′	3732m	3744	3723	3927	3562	(N-H) υ	**58**
3	A′	3606w	3618	3597	3806	3453	(N-H) υ	**54**
4	A′	-	3618	3597	3806	3453	(N-H) υ	**54**
5	A′	3415m	3527	3507	3805	3452	(N-H) υ	**100**
6	A′	3323w	3236	3217	3380	3066	(C-H) υ	**96**
7	A′	-	3228	3209	3376	3063	(C-H) υ	**79**
8	A′	-	3220	3201	3368	3055	(C-H) υ	**96**
9	A′	-	3214	3196	3360	3048	(C-H) υ	**81**
10	A′	-	3211	3193	3356	3044	(C-H) υ	**73**
11	A′	-	3193	3175	3338	3028	(N-H) υ	**96**
12	A″	-	3191	3173	3337	3027	(C-H) υ	**86**
13	A″	3157vs	3184	3166	3321	3013	(C-H) υ	**95**
14	A″	-	1774	1764	1920	1742	(O=C) υ	**79**
15	A″	-	1772	1762	1914	1736	(O=C) υ	**78**
16	A″	-	1674	1664	1822	1653	(C=C) υ	**18**
17	A″	1656vs	1671	1661	1795	1628	(C=C) υ	**20**
18	A″	-	1644	1634	1780	1614	(C-C) υ	**19**
19	A″	-	1633	1623	1774	1609	(C-C) υ	**28**
20	A″	-	1622	1612	1772	1607	(N-H) δ	**75**
21	A″	1604s	1620	1610	1761	1597	(N-H) δ	**76**
22	A″	-	1578	1569	1750	1587	(N-N) υ	**25**
23	A″	-	1561	1552	1696	1538	(N-N) υ	**47**
24	A″	1525s	1542	1533	1671	1516	(H-C) δ	**17**
25	A′	-	1519	1510	1652	1498	(H-N) δ	**22**

26	A′	-	1455	1446	1556	1411	(C-C) υ	**27**
27	A′	-	1453	1444	1551	1407	(C-C) υ	**24**
28	A′	1392vs	1389	1381	1473	1336	(N-C) υ	**22**
29	A′	-	1385	1377	1471	1334	(N-C) υ	**21**
30	A′	-	1373	1365	1455	1320	(C-C) υ	**11**
31	A′	-	1369	1361	1443	1309	(C-C) δ	**12**
32	A′	-	1336	1328	1380	1252	(H-C) δ	**31**
33	A′	1307m	1325	1317	1340	1215	(C-H) δ	**26**
34	A′	1275vs	1287	1279	1333	1209	(H-N) δ	**25**
35	A′	-	1267	1259	1294	1174	(H-N) δ	**38**
36	A′	-	1240	1233	1286	1166	(N=N) υ	**32**
37	A′	1199vs	1198	1191	1282	1163	(H-C) δ	**28**
38	A′	1168vs	1186	1179	1266	1148	(C-H) δ	**28**
39	A′	-	1155	1148	1233	1118	(C-C) υ	**17**
40	A′	-	1153	1146	1232	1117	(C-C) υ	**18**
41	A′	-	1139	1132	1195	1084	(C-H) δ	**25**
42	A′	-	1133	1126	1186	1076	(C-H) δ	**17**
43	A′	-	1095	1088	1180	1070	(H-N) δ	**43**
44	A′	-	1094	1087	1175	1066	(H-N) δ	**43**
45	A′	-	1033	1027	1109	1006	(C-C) δ	**41**
46	A′	-	1031	1025	1105	1002	(C-C) δ	**37**
47	A″	-	1003	997	1101	998	(CC) τ	**46**
48	A″	-	988	982	1099	997	(CC) τ	**61**
49	A″	-	974	968	1081	980	(CC) τ	**43**
50	A″	-	970	964	1079	978	(CC) τ	**50**
51	A′	-	960	954	1019	924	(N-N) δ	**15**
52	A″	-	883	878	970.4	880	(CC) τ	**33**
53	A″	-	861	856	943.4	855	(CC) τ	**27**
54	A′	850s	856	851	937.5	850	(C-C) δ	**12**
55	A″	-	847	842	915.3	830	(CC) τ	**32**
56	A″	-	831	826	901.2	817	(CC) τ	**37**
57	A″	-	792	787	866.9	786	(NC) γ	**37**
58	A″	779s	783	778	859.7	780	(NC) γ	**39**
59	A′	-	780	775	830.0	753	(C-C) υ	**10**
60	A′	725m	732	727	782.2	709	(C-C) υ	**10**
61	A″	-	718	713	779.6	707	(C-C) τ	**26**
62	A″	-	715	710	776.0	704	(C-C) τ	**23**
63	A′	-	648	644	697	632	(C-C) δ	**15**
64	A′	-	638	634	690	626	(OCN) δ	**21**
65	A″	-	632	628	680	616	(C-C) γ(C-N) γ	**13**
66	A″	613m	629	625	622	564	(N-N) τ	**85**
67	A′	567m	576	572	602	546	(CN) δ	**14**
68	A″	-	558	554	593	538	(N-C) τ	**38**
69	A″	-	548	544	561	508	(N-C) τ	**54**
70	A″	-	523	520	559	507	(N-C) τ	**23**
71	A′	-	513	510	539	489	(NCC) δ	**21**
72	A′	-	491	488	531	481	(NCC) δ	**32**
73	A″	-	483	480	514	466	(C-C) γ	**21**
74	A″	-	444	441	475	430	(NCC) γ	**12**

75	A″	-	422	419	461	418	(C-C) τ	**23**
76	A″	-	418	415	455	412	(C-C) τ	**32**
77	A′	-	409	406	439	398	(C-N) δ	**17**
78	A″	-	380	377	438	397	(N-C) τ	**68**
79	A″	-	377	374	435	394	(N-C) τ	**68**
80	A″	-	341	339	370	335	(N-C) τ	**16**
81	A″	-	340	338	363	329	(N-N) τ	**11**
82	A″	-	286	284	301	273	(C-C) γ	**25**
83	A′	-	249	247	269	244	(CCC) δ	**16**
84	A′	-	218	216	235	213	(CCC) δ	**16**
85	A″	-	216	214	232	210.	(N-N) τ	**26**
86	A′	-	178	177	189	171	(CCC) δ	**14**
87	A″	-	173	172	155	140	(N-N) τ	**40**
88	A′	-	126	125	136	123	(NCC) δ	**19**
89	A″	-	113	112	112	101	(C-C) τ	**24**
90	A″	-	63	63	69	62	(C-C) τ	**77**
91	A″	-	63	62	67	60	(C-C) τ	**64**
92	A″	-	57	56	56	50	(C-C) τ	**22**
93	A′	-	35	35	36	32	(NNC) δ	**26**
94	A″	-	25	25	18	16	(N-C) τ	**56**
95	A″	-	9	9	8	7	(C-C) τ	**68**
	a			0.997		0.958		
	b			5.992		14.04		
	R^2			0.998		0.996		
	$Freq_{exp.} = a\ Freq_{theo.} + b$							

vs – very strong; s – strong; m – medium; w – weak; υ – stretching; δ – in plane bending; γ – out plane bending; τ- Torsion.

3.2.1. C-H vibrations

The aromatic structure displays the presence of the C-H stretching vibrations in the region 3000–3100 cm^{-1} which is the characteristic region for the ready identification of the C-H stretching vibrations (Fereyduni *et al*., 2011). In this region, the bands are not affected considerable by the nature of the substituent. The wavenumber 3157 cm^{-1} is assigned to C-H stretching vibration of the phenyl groups. This peak is predicted at 3166 cm^{-1} at PBE1PBE/6-311+G(2d,p) and 3013cm^{-1} at HF/6-311+G(2d,p) (mode no.13). As indicated by the PED, this mode involves the contribution of 95%. The scaled vibrations by PBE1PBE/6-311+G(2d,p), method shows very good agreement with recorded spectral data. The aromatic C–H in-plane bending and out-of-plane bending vibrations naturally occur in the region 300–1000 cm^{-1} and 750-1000 cm^{-1} respectively (Krishnakumar *et al*., 2008), the bands are sharp but have been weak-to medium intensity. In this present case, the in-plane bending of phenyl ring computed at 1533, 1317,1191 and 1179 cm^{-1} at the PBE1PBE/6-311+G(2d,p) level matches with 1525, 1307,1199 and 1168 cm^{-1} in IR (mode no.24,33, 37, 38). The PED, these modes involves the contribution of 17%, 26% and 28%. The C-H vibrations band is in the expected region and it is with almost strong intensity; hence there is a benzene structure.

3.2.2. C=C Vibrations

The present molecule consists of two benzene rings, there are six C=C stretching vibrations are possible. In this work, the frequency experimentally observed in the FT-IR spectrum at 1656 cm^{-1} which it assigned to the C=C stretching vibrations (mode no. 17). The theoretically computed value at the PBE1PBE/6-311+G(2d,p) and HF/6-311+G(2d,p) levels indicated the peaks at 1661 cm^{-1} and 1628 cm^{-1}, respectively with the contribution of 20%. Thus, the PBE1PBE method showed satisfactory agreement with experimental value. Besides, the ring C=C stretching vibrations would affect as a result of the bonding of N=N in the ring.

3.2.3. C-C Vibrations

In the present case, the C–C stretching vibrations observed at 725 cm^{-1} (mode no. 60). The theoretically computed value at the PBE1PBE/6-311+G(2d,p) and HF/6-311+G(2d,p) levels indicated the peaks at 727 cm^{-1} and 709 cm^{-1}, respectively with the contribution of 10%. The closer calculated frequency is at 727 cm^{-1} devoted to the RPBE1PBE/6-311+G(2d,p) method. In the present work, the strong band presents at 850 cm^{-1} assigned to the C–C–C in-plane bending (mode no.54). The theoretically computed value at the PBE1PBE/6-311+G(2d,p) and HF/6-311+G(2d,p) levels showed the peaks at 851 cm^{-1} and 850 cm^{-1}, respectively with the contribution of 12%.

3.2.4. N=N and N-N Vibrations

For azo groups we cannot observe N=N stretching, N-N stretching, N=N-N-ring in-plane. Only observed the N-N out-of-plane bending vibration is at 613cm^{-1} mode no. 66. The calculated frequencies were at 625 cm^{-1} and 564 cm^{-1} using the RPBE1PBE/6-311+G (2d,p) and HF/6-311+G(2d,p) levels, respectively. As indicated by the PED, this mode (mode no. 66) involves the contribution of 85%.

3.2.5. N-H and C-N Vibrations

A band is experimentally observed at 3606 cm^{-1} in the FT-IR spectrum which assigned to the N–H stretching vibration. The theoretical wavenumber of the N–H stretching vibration (mode no. 3) is at 3597 cm^{-1} and 3453 cm^{-1} using the RPBE1PBE/6-311+G(2d,p) and HF/6-311+G(2d,p) levels, respectively. The PED confirms that this mode of vibration have the contribution of 54%.

The identification of C–N vibrations are very challenging, because of combining several bands are probable in this region (Sundaraganesan *et al*., 2009) determined the C–N stretching absorption in 1266–1382 cm^{-1} for aromatic amines. In benzamide the band observed is assigned at 1368 cm^{-1}(Shunmugam *et al*., 1984). The strong band is observed at 1392 for the C-N stretching vibrations (mode no. 28). The calculated frequencies were at 1381 cm^{-1} and 1336 cm^{-1} using the RPBE1PBE/6-311+G(2d,p) and HF/6-311+G(2d,p) levels, respectively. The band observed at 779 cm^{-1} is related to the C-N out of plan bending (mode no. 58) which the theoretically wavenumber was at 778 cm^{-1} and at 780 cm^{-1} using RPBE1PBE/6-311G+(2d,p) and HF/6-311G+(2d,p) levels, respectively. As indicated by the PED, the two modes (modes no. 28 and 58) involve the contribution of 22% and 39%, respectively. All the vibrations are shifted down due to the suppression of the N=N moiety.

3.2.6. $CONH_2$ Vibrations

In present study, the C=O stretching vibration was observed in the FT-IR at 3157 cm^{-1} (mode no. 13). The PED of this mode involves the contribution of 95%. The computed wavenumber for this mode occurred at 3166 cm^{-1} at the RPBE1PBE/6-311+G(2d,p) level which is in good agreement with the experimental value. The NH_2 group has two NH stretching vibrations, one being asymmetric and the other symmetric. The frequency of asymmetric vibration is generally greater than symmetric one. In our study, the strong bands observed at 3732 cm^{-1} and 3415 cm^{-1} in the FT-IR are assigned to asymmetric and symmetric stretching vibrations respectively. The theoretically scaled wavenumbers were at 3723 cm^{-1} and 3507 cm^{-1} using RPBE1PBE/6-311+G (2d,p) level which assigned to the asymmetric and symmetric amino stretching vibrations, respectively (modes no. 2 and 5). These peaks were predicated at 3562 cm^{-1} and 3452 cm^{-1} using HF/6-311G+(2d,p) level. As indicated by the PED, these modes involve the contribution of 58% and 100%, respectively.

4. CONCLUSIONS

The title compound was synthesized via reaction of 4-aminobenzamide and sodium nitrite in acidic solution. The structure was determined and characterized by FT-IR, ^{1}H and ^{13}C NMR. The molecular geometries, harmonic vibrational frequencies of **2** are determined and analyzed by HF and DFT (RPBE1PBE) with 6-311+G(2d,p) basis set. Comparison between the calculated optimized geometry and the experimental values indicates that the RPBE1PBE/6-311+G(2d,p) method can predict the bond length, bond angle and dihedral angles of the **2** better than HF/6-311+G(2d,p) method. The Calculated vibrational wavenumbers and the experimental FT-IR spectra agreeably support each other. The difference between the observed and scaled wavenumber values of most of fundamentals is very small.

ACKNOWLEDGMENT
Islamic Azad University, Miyaneh Branch was gratefully acknowledged for their financial support.

REFERENCES

Abdel-Shafy H., Perlmutter H. and Kimmel H. (1977). Vibrational studies of monosubstituted halogenated pyridines. *J. Mol. Struct*. 42:37–49.

Domingues V.O., Hörner R., Reetz L.G.B., Kuhn F., Coser V.M., Rodrigues J.N., Bauchspiess R., Pereira W.V., Paraginski G.L., Locatelli A., Fank J.O., Giglio V.F. and Hörner M. (2010). In vitro evaluation of triazenes: DNA cleavage, antibacterial activity and cytotoxicity against acute myeloid leukemia cells. *J. Braz. Chem. Soc*. 21:2226–2237.

Enders D., Rijksen C., Köbberling E.B., Gillner A. and Köbberling, J. (2004). A triazene-based new photolabile linker in solid phase chemistry. *Tetrahedron Lett.* 45:2839–2841.

Erdogdu Y., Gulluoglu M.T. and Kurt M. (2009). Analysis of vibrational spectra of 2 and 3-methylpiperidine based on density functional theory calculations. *J. Raman Spectrosc.* 40:1615–1623.

Fereyduni E., Vessally E., Yaaghubi E. and Sundaraganesan N. (2011). One-pot synthesis, FT-IR, NMR and density functional method (B3LYP) studies on 2-(cyclohexylamino)-2-oxo-1-(pyridin-2-yl) ethyl benzoate. *Spectrochimica Acta Part A.* 81:64–71.

Frisch M.J. et al. (2004). Gaussian 03, Revision B.05, Gaussian, Inc., Wallingford, CT.

Griess P. (1859). On a new series of bodies in which nitrogen is substituted for hydrogen. Proc. Royal Soc. London .9: 594–597.

Iglesias B.A., Hörner M., Toma H.E. and Araki K. (2012). 5-(1-(4-phenyl)-3-(4-nitrophenyl) triazene)-10, 15, 20-triphenylporphyrin: a new triazene-porphyrin dye and its spectroelectrochemical properties. *J. Porphyrins Phthalocyanines.*16:200–209.

Kimball D.B., Herges R. and Haley M.M. (2002). Two unusual, competitive mechanisms for (2-ethynylphenyl) triazene cyclization: Pseudocoarctate versus pericyclic reactivity. *J. Am. Chem. Soc.* 124:1572–1573.

Krishnakumar V., Prabavathi N. and Muthunatesan S. (2008). Density functional theory study of vibrational spectra, and assignment of fundamental vibrational modes of 1-bromo 4-fluoronaphthalene. *Spectrochim. Acta A.* 70:991–996.

Melardi M.R., Aghamohamadi M., Gharamaleki J.A., Rofouei M.K. and Notash, B. (2012). 1-(3, 5-Dichlorophenyl)-3-(2-methoxyphenyl) triaz-1-ene. *Acta Cryst.* E68, 724.

Merrick P.J., Moran D. and Radom L. (2007). An evaluation of harmonic vibrational frequency scale factors. *J. Phys. Chem. A.* 111:11683-11700

Morgan K.J. (1961). Infrared spectra and structure of arylazonaphthols. *J. Chem. Soc.* 2151–2159.

Rofouei M.K., Gharamaleki J.A., Fereyduni E., Aghaei A., Bruno G., Rudbari H.A. and Anorg. Z. (2012). Synthesis, characterization and crystal structures of Hg II complexes with asymmetric ortho-functionalized 1, 3-bis (aryl) triazenide ligands. *Allg. Chem.* 638:220–223.

Sanada M., Takagi Y., Ito R. and Sekiguchi, M. (2004). Killing and mutagenic actions of dacarbazine, a chemotherapeutic alkylating agent, on human and mouse cells: effects of Mgmt and Mlh1 mutations. *DNA Repair*. 3:413–420.

Santos A.J.R., Bersch P., Oliveira H.P.M., Hörner M. and Paraginski G.L. (2014). In vitro antibacterial activity and toxicity toward Artemia salina Leach of some triazene compounds. *J. Mol. Struct.* 1060:264–271.

Shunmugam R. and Sathyanarayana D. N. (1984). Raman and polarized infrared spectra of pyridine-2-thione. *Spectrochim. Acta A.* 40:757-761.

Sundaraganesan N., Karpagam J., Sebastian S. and Cornard J.P. (2009). The spectroscopic (FTIR, FT-IR gas phase and FT-Raman), first order hyperpolarizabilities, NMR analysis of 2,4-dichloroaniline by ab initio HF and density functional methods. *Spectrochimica Acta Part A.* 73:11–19.

Vessally E., Fereyduni E., Erdogdu Y., Habibi A., Eskandari K. and Gulluoglu M.T. (2011). One-pot synthesis, FT-IR, NMR and density functional method (B3LYP) studies on 2-(cyclohexylamino)-2-oxo-1-(pyridin-2-yl) ethyl benzoate. *J. Mol. Struct*. 985:120–127.

